In Vitro Evidence for the Dual Function of Alg2 and Alg11: Essential Mannosyltransferases in N-Linked Glycoprotein Biosynthesis†

Mary K. O'Reilly,‡ Guofeng Zhang,‡ and Barbara Imperiali*,‡,§

Departments of Chemistry and Biology, Massachusetts Institute of Technology, Cambridge, Massachusetts 02139

Received May 3, 2006; Revised Manuscript Received June 13, 2006

ABSTRACT: The biosynthesis of asparagine-linked glycoproteins utilizes a dolichylpyrophosphate-linked glycosyl donor (Dol-PP-$GlcNAc_2Man_9Glc_3$), which is assembled by the series of membrane-bound glycosyltransferases that comprise the dolichol pathway. This biosynthetic pathway is highly conserved throughout eukaryotic evolution. While complementary genetic and bioinformatic approaches have enabled identification of most of the dolichol pathway enzymes in *Saccharomyces cerevisiae*, the roles of two of the mannosyltransferases in the pathway, Alg2 and Alg11, have remained ambiguous because these enzymes appear to catalyze only two of the remaining four unannotated transformations. To address this issue, a biochemical approach was taken using recombinant Alg2 and Alg11 from *S. cerevisiae* and defined dolichylpyrophosphate-linked substrates. A cell-membrane fraction isolated from *Escherichia coli* overexpressing thioredoxin-tagged Alg2 was used to demonstrate that this enzyme actually carries out an α1,3-mannosylation, followed by an α1,6-mannosylation, to form the first branched pentasaccharide intermediate of the pathway. Then, using thioredoxin-tagged Alg2 for the chemoenzymatic synthesis of the dolichylpyrophosphate pentasaccharide, it was thus possible to define the biochemical function of Alg11, which is to catalyze the next two sequential α1,2-mannosylations. The elucidation of the dual function of each of these enzymes thus completes the identification of the entire ensemble of glycosyltransferases that comprise the dolichol pathway.

On the pathway of asparagine-linked protein glycosylation, a dolichylpyrophosphate-linked tetradecasaccharide composed of *N*-acetyl-D-glucosamine (GlcNAc),[1] D-mannose (Man), and D-glucose (Glc) monosaccharides ($Glc_3Man_9GlcNAc_2$-PP-Dol) is biosynthesized at the endoplasmic reticulum (ER) membrane by a series of glycosyltransferases that comprise the dolichol pathway (*1*). This process is highly conserved among all eukaryotes, culminating in the oligosaccharyltransferase-mediated cotranslational transfer of the tetradecasaccharide to nascent polypeptides (*2*, *3*). As a result of more than 2 decades of genetic screening for yeast mutants deficient in donor assembly, supplemented by biochemical studies as well as bioinformatic approaches, nearly all of the genes of this pathway in *Saccharomyces cerevisiae* have been annotated (*4*−*8*). The first seven steps of the dolichol pathway are known to occur on the cytoplasmic face of the ER membrane, while the remaining seven take place on the lumenal face of the membrane (*9*, *10*). Translocation of the heptasaccharide intermediate to the lumen is facilitated by Rft1 through an unknown mechanism (*11*).

Alg7, which catalyzes the first committed step of the pathway, mediates the coupling of GlcNAc-1-phosphate from uridine 5′-diphospho-*N*-acetyl-α-D-glucosamine (UDP-GlcNAc) with dolichyl-phosphate to yield GlcNAc-PP-Dol (*12*). This intermediate then acts as a substrate for the Alg13/14 heterodimeric complex that transfers a second GlcNAc from a UDP-GlcNAc donor (*7*, *13*, *14*). The first mannosyl transfer step is carried out by Alg1 using guanosine 5′-diphospho-α-D-mannose (GDP-Man) as the glycosyl donor (*15*−*17*). This mannosyltransferase has been well-characterized in vitro, attracting particular attention because of the challenge of preparing β1,4-mannosides by chemical synthesis (*18*−*21*). For the final four cytosolic mannosylation steps, which also use GDP-Man as the glycosyl donor, only two candidate enzymes have been identified. It has been suggested that Alg2 is responsible for either the second, third, or both the second and third mannosylation steps (*22*−*26*) and that Alg11 is responsible for either the fourth, fifth, or both the fourth and fifth mannosylation steps (*3*, *5*, *27*). Recently, the use of bioinformatic tools has greatly facilitated the identification of "missing" enzymes in the dolichol pathway such as Alg12 and Alg13/14 (*7*, *28*); however, no candidates have been put forward for the remaining mannosyltransferase activities. This situation suggested that perhaps Alg2 and/or Alg11 could be responsible for more than one biosynthetic step (Figure 1). It is noteworthy that

† This work was supported in full by the NIH Grant GM68692.

* To whom correspondence should be addressed. Telephone: 1-617-253-1838. Fax: 1-617-452-2419. E-mail: imper@mit.edu.

‡ Department of Chemistry.

§ Department of Biology.

[1] Abbreviations: 2-AB, 2-aminobenzamide; ALG, asparagine-linked glycosylation; Dol-PP, dolichylpyrophosphate; ER, endoplasmic reticulum; GDP-Man, guanosine 5′-diphospho-α-D-mannose; Glc, D-glucose; GlcNAc, *N*-acetyl-D-glucosamine; HPLC, high-performance liquid chromatography; MALDI−MS, matrix-assisted laser desorption ionization−mass spectrometry; Man, D-mannose; TMHMM, transmembrane prediction using hidden Markov models; TFA, trifluoroacetic acid; TRX, thioredoxin; UDP-GlcNAc, uridine 5′-diphospho-*N*-acetyl-α-D-glucosamine.

10.1021/bi060878o CCC: $33.50
Published on Web 07/14/2006

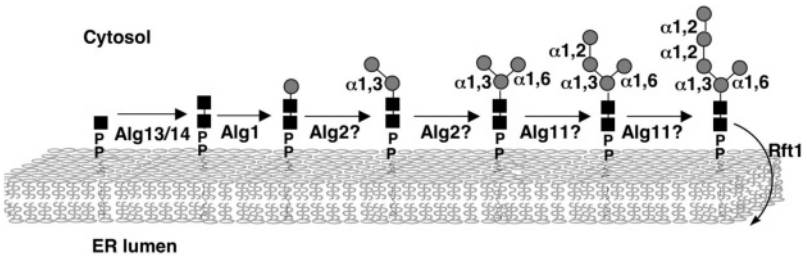

FIGURE 1: Elongation of the GlcNAc-PP-Dol intermediate to $Man_5GlcNAc_2$-PP-Dol on the cytosolic side of the ER membrane, by the indicated glycosyltransferases, prior to translocation to the lumenal face. Gray circles are mannose residues (Man); black squares are *N*-acetylglucosamine residues (GlcNAc); P represents a phosphate group; and dolichyl moieties embedded within the membrane.

dual functionality was recently substantiated for Alg9, which carries out two α1,2-mannosylation steps in the ER lumen, adding the seventh and ninth mannose residues (*8*).

Although Alg2 mutants have been identified and characterized in *S. cerevisiae* (*22*), *Rhizomucor pusillus* (*25*), and human (*26*), the characterization of each has yielded varied results. Yeast mutants isolated included point mutations in *ALG2* conferring temperature sensitivity, while nucleotide deletion or insertion in the human and fungal *ALG2* mutant genes, respectively, led to truncated gene products in both cases. In the expressed products of the yeast and human *ALG2* mutant genes, the sequence of Alg2 was not affected in the conserved signature sequence that is shared by a number of other glycosyltransferases involved in a wide range of functions in carbohydrate metabolism, including Alg11 and MurG. MurG is an enzyme with a role in bacterial cell-wall biosynthesis that is analogous to Alg13/Alg14 (*29*). In the Alg2 sequence, as well as Alg11 and many other glycosyltransferases from the same Pfam family (*30*), the signature sequence also contains a conserved EX_7E motif. Interestingly, Alg2 and Alg11 share 22% homology overall. In contrast to the truncated gene product of the human Alg2 mutant, which retains the signature sequence, the consequence of the 5-bp insertion found in *ALG2* of the filamentous fungi, *R. pusillus*, mutant is a more severe truncation of Alg2 that results in a loss of the signature sequence.

Metabolic labeling with [^{3}H]Man of the mutant yeast strain or fibroblasts from the human patient with the *ALG2* mutation revealed an accumulation of dolichylpyrophosphate-linked tris- and tetrasaccharides (*22*, 26), whereas the fungal mutant, lacking the signature sequence, accumulated only the trisaccharide intermediate (*25*). Interestingly, *ALG2* is not an essential gene in *R. pusillus* and, because of the severity of the mutation described in this study, may in effect represent an *ALG2* deletion strain. These results suggested a role for Alg2 in the second mannose transfer step but were not able to reveal information about the putative role of Alg2 in the following step.

The yeast mutant, *alg11*, was isolated on the basis of resistance to sodium vanadate and was shown to affect glycosylation at an early step in the pathway (*5*). Efforts to define the precise step for which Alg11 is responsible included extensive characterization of dolichylpyrophosphate-linked saccharide intermediates and glycoproteins extracted from *alg11* mutant cells (*5*). These data suggested that Alg11 catalyzes the fifth mannosylation, which is the seventh step in the pathway and the last step prior to translocation to the lumen; however, interpretation of these results was difficult because of the nonspecific translocation by Rft1 and elongation by the lumenal glycosyltransferases. While thorough genetic studies have been valuable for narrowing down the functions of Alg2 and Alg11, in vitro biochemical validation is critical for unambiguously defining the precise roles of these mannosyltransferases in the pathway.

Alg2 from *S. cerevisiae* is a 58-kDa mannosyltransferase including four predicted transmembrane domains that are grouped into two pairs of closely spaced domains, with one pair at the C terminus and the other pair located near the N terminus, as predicted by the TMHMM server, version 2.0 (*31*). Alg11 from *S. cerevisiae* is a 63-kDa protein with one predicted transmembrane domain at the N terminus, as predicted by the TMHMM server, version 2.0 (*31*). In this study, Alg2 and Alg11 were cloned and expressed in *Escherichia coli* as thioredoxin (TRX) fusions at the N terminus for improved expression. To evaluate the mannosyltransferase activity of each of these enzymes, the trisaccharide intermediate, $ManGlcNAc_2$-PP-Dol, was first prepared by a chemoenzymatic approach using recombinant Alg1 isolated from overexpression in *S. cerevisiae*. The cell-membrane fractions containing overexpressed TRX-Alg2 or TRX-Alg11 were used to demonstrate that Alg2 catalyzes the elongation of the trisaccharide $ManGlcNAc_2$-PP-Dol to $Man_3GlcNAc_2$-PP-Dol and that Alg11 catalyzes the elongation of the pentasaccharide product of TRX-Alg2 to the heptasaccharide intermediate, $Man_5GlcNAc_2$-PP-Dol. These results resolve a longstanding uncertainty regarding the exact roles of Alg2 and Alg11 in the dolichol pathway.

EXPERIMENTAL PROCEDURES

Cloning of ALG1, ALG2, and ALG11 Constructs. ALG1, *ALG2*, and *ALG11* were all amplified from yeast genomic DNA by polymerase chain reaction (PCR) using Vent polymerase. The genomic DNA was extracted from the *S. cerevisiae* strain PRY46 using the yeast DNA extraction reagent (Y-DER) (Pierce, Inc.). Each gene was cloned into the pENTR/SD/D-TOPO "entry" vector (Invitrogen) and then transferred to a "destination" vector for expression in either *E. coli* (pBAD-DEST49) or *S. cerevisiae* (pYES-DEST52) by homologous recombination using Gateway Cloning Technology (Invitrogen). All mutants were prepared by site-directed mutagenesis of clones in pENTR vectors (prior to homologous recombination). The *ALG2* double mutant was prepared by changing the codon corresponding to E343A in the E335A mutant background, while the *ALG11* double mutant was prepared by incorporating both mutations simultaneously in the wild-type background. All pENTR clones were verified by DNA sequencing at the Biopolymers Laboratory of the MIT Center for Cancer Research. Details of the cloning procedures can be found in the Supporting Information.

Expression in S. cerevisiae and Purification of Alg1. Alg1-V5-His was expressed from the vector pYES(*ALG1*)-DEST52 in the yeast strain INV*Sc*1. Solubilized microsomes were prepared by differential centrifugation and further purified by Ni−NTA chromatography to yield 0.26 mg of Alg1 from a 4 L expression culture, with a specific activity of 1.8 μmol h^{-1} mg^{-1} ($\pm$0.99 μmol h^{-1} mg^{-1} based on four assays), with a fixed concentration of 2 μM GDP-Man. Assays were run as described previously (*32*), and the specific activity refers to micromoles of [^{3}H]Man transferred from GDP-[^{3}H]Man to the dolichylpyrophosphate-linked substrate by 1 mg of Alg1 in 1 h. Details of the expression and purification can be found in the Supporting Information.

Preparation of Dol-PP-GlcNAc$_2$Man with Alg1 Expressed in S. cerevisiae. To a dried aliquot of approximately 15−20 nmol of GlcNAc$_2$-PP-Dol, 500 μL of buffer A [38 mM Tris-HCl at pH 7.2, 1.8 mM dithiothreitol (DTT), 0.28 mM ethylenediaminetetraacetic acid (EDTA), and 0.26% NP-40] was added and sonicated for 1 min to disperse the substrate. The reaction mixture was then brought to 2 mM GDP-Man and 10 mM $MgCl_2$ and a final volume of 990 μL with dH_2O. A 10 μL aliquot of Alg1 (2.5 μM) was added to initiate the reaction. The reaction mixture was incubated at 37 °C for 1 h and then quenched by the addition to 11 mL of $CHCl_3$/MeOH/4 mM aqueous $MgCl_2$ (6:4:1). The organic phase was washed twice with 2 mL of $CHCl_3$/MeOH/4 mM $MgCl_2$ (2.75:44:53.25), then evaporated to dryness, redissolved in 1 mL of $CHCl_3$/MeOH (3:2), and aliquoted (10 μL/tube). Aliquots were redried and stored at −80 °C. The amount of dolichylpyrophosphate-linked substrate is difficult to quantify, but a rough approximation was made by comparing the peak size on the fluorescence-detected high-performance liquid chromatography (HPLC) to a known amount of maltotriose, labeled with 2-aminobenzamide (2-AB) and separated from unreacted 2-AB in the same way as the hydrolyzed glycan sample.

Protein Expression and Preparation of E. coli Membranes. For *E. coli* expression, One Shot Top 10 competent cells were transformed with either pBAD(*ALG2*)-DEST49 or pBAD(*ALG11*)-DEST49 together with plasmid isolated from BL21(DE3)RIL codon-plus competent cells (Stratagene) to enhance the translation of rare codons. Both plasmids were selected on the basis of the carbenicillin resistance of pBAD-DEST49 and chloramphenicol resistance of the codon-plus plasmid. A 10 mL portion from an overnight culture was added to 2.5 L of Terrific Broth (Invitrogen) and grown at 37 °C with shaking to an OD_{600} of 0.8−1.0. The culture was then adjusted to 16 °C prior to the induction of protein expression with the addition of L-arabinose to 0.2% (w/v). After 24 h, cells were harvested at 4 °C by centrifugation (25 min, 5000*g*), washing once with 0.9% (w/v) NaCl. The resulting pellet was either taken forward to cell-membrane preparation immediately or stored at −80 °C until use. To prepare the membrane fraction, all steps were performed at 4 °C. Cell pellets from 2.5 L expressions were resuspended in 50 mL of buffer B (50 mM Tris-acetate at pH 8.5 and 1 mM EDTA) containing 1× protease inhibitor cocktail III (Calbiochem). Cells were lysed by sonication and centrifuged for 30 min at 5700*g*. The membrane fraction was pelleted by centrifugation of the supernatant for 1 h at 142400*g*. The resulting pellet was rinsed with buffer B, then homogenized in 0.5 mL of buffer B, and stored at −20 °C in 30% (v/v) glycerol.

Elongation of Dolichyl-Linked Saccharide Intermediates. Reaction mixtures were approximately 40 μM dolichylpyrophosphate-linked starting material, 2 mM GDP-Man, and 2.0 or 1.4 μg/μL (total protein) of membrane fraction containing TRX-Alg2 or TRX-Alg11, respectively. Starting with a dried aliquot of the dolichylpyrophosphate-linked starting material, a 50-μL aliquot of buffer A was added and the mixture was sonicated for 1 min to resuspend the substrate. The reaction mixture was then brought to 2 mM GDP-Man and 10 mM $MgCl_2$, and dH_2O was added, anticipating a final volume of 100 μL. The membrane fraction (5 μL) containing either TRX-Alg2 or TRX-Alg11 was added to initiate the reaction. Incubation proceeded for 1 h at room temperature, followed by quenching into a biphasic mixture of $CHCl_3$/MeOH/4 mM $MgCl_2$ (6:4:1). The dolichylpyrophosphate-linked saccharides, which partitioned into the organic phase, were subsequently washed twice with 200 μL aliquots of $CHCl_3$/MeOH/4 mM $MgCl_2$ (2.75:44:53.25) or $CHCl_3$/MeOH/100 mM KCl (3:48:47) (the latter was used for larger saccharides such as the Alg11 products). The extracted organic phase was then concentrated to dryness, resuspended in 0.5 mL of *n*-propanol/0.2 M trifluoroacetic acid (TFA) (1:1), and heated to 50 °C for 15 min to hydrolyze glycans from the dolichyl pyrophosphate. Hydrolysis products were then evaporated to dryness.

2-AB Labeling of Saccharides (33). To prepare the fluorescent-labeling reagent, a 150 μL aliquot of acetic acid was added to a 350 μL aliquot of dimethyl sulfoxide and then a 100 μL aliquot of this mixture was used to dissolve 5 mg of 2-AB. The entire dye solution was added to 6 mg of sodium cyanoborohydride and mixed well to dissolve the reductant. Aliquots of 5 μL of this reagent were then added to dried samples of hydrolyzed, dried glycans and heated to 65 °C for 2−4 h. Postlabeling cleanup was accomplished by using GlykoClean S cartridges (ProZyme, Inc.) according to the protocol of the manufacturer.

Normal-Phase HPLC (34). The normal-phase analytical HPLC column (GlykoSepN) was purchased from ProZyme, Inc. The solvents used were 50 mM ammonium formate at pH 4.4 (solvent A) and acetonitrile (solvent B). A linear gradient of 20−52% solvent A in solvent B over 80 min was used to elute the 2AB-labeled glycans. Labeled glycans were detected with a Waters scanning fluorescence detector (λ_{ex}, 330 nm; λ_{em}, 420 nm). For standardization of the column, every dolichylpyrophosphate-linked intermediate from GlcNAc to Man$_5$GlcNAc$_2$ was prepared as the hydrolyzed and derivatized species, analyzed by HPLC, and confirmed by matrix-assisted laser desorption ionization−mass spectrometry (MALDI−MS). Mono- and disaccharides were hydrolyzed from synthetic preparations; the trisaccharide was hydrolyzed from the chemoenzymatic Alg1 preparation; and tetra- through heptasaccharides were obtained by elongating the trisaccharide intermediate using microsomes from wild-type yeast (INV*Sc*1, Invitrogen) as well as a temperature-sensitive *alg11* yeast strain (NDY 13.4) (*35*). Typically 5−20 pmol of material was injected for HPLC analysis.

MALDI. Mass spectrometric analysis was performed on a PE Biosystems Voyager System 4028 using the reflector, positive mode as described (*36*). Calibration mixture #1 from

the Sequazyme mass standards kit (Applied Biosystems) was used for standardization.

Mannosidase Cleavage. 2-AB-labeled glycans were collected from HPLC separation and then concentrated to dryness using a Sc110 Speed-Vac (Savant, Inc.). For characterization of the TRX-Alg2 products, dried glycans were redissolved in 5 μL of dH_2O and 1 μL aliquots were treated with 2 units (1 μL) of α1−2,3-mannosidase from *Xanthomonas manihotus* (New England BioLabs, Inc.) in 50 mM sodium citrate at pH 6.0, 5 mM $CaCl_2$, and 100 mg/mL bovine serum albumin (BSA), or with 1 milliunit (1 μL) of α1,6-mannosidase from *Xanthomonas* sp. (Calbiochem) in 50 mM sodium phosphate at pH 5.0 and 37 °C for 5 h. For the α1−2,3-mannosidase reactions, 0.5 μL aliquots each of commercial buffer (10×) and BSA (10×), which were supplied with the enzyme, were used in a final reaction volume of 5 μL. α1,6-Mannosidase reactions were performed in a final volume of 10 μL, using 1× buffer.

For characterization of the TRX-Alg11 wild-type and mutant products, α1,2-mannosidase from *Aspergillus saitoi* was purchased from ProZyme, Inc. and reconstituted according to the instructions of the manufacturer. Briefly, at 4 °C, 16 μL of dH_2O was mixed with 4 μL of 5× reaction buffer provided by the manufacturer to make a 1× reaction buffer. Then, 10 μL of the 1× reaction buffer was slowly added to the vial containing the dried enzyme and mixed by gentle pipeting followed by a brief centrifugation. The reconstituted enzyme was stored at 4 °C. For cleavage reactions, dried glycan fractions ($Man_4GlcNAc_2$-2AB or $Man_5GlcNAc_2$-2AB collected from HPLC) were redissolved into 5 μL of dH_2O and 1 μL of heptasaccharide or 2 μL of hexasaccharide was mixed with 1.8 μL of 5× reaction buffer, dH_2O (7.2 or 6.2 μL for the hepta- and hexasaccharide cleavages, respectively), and 1 μL of reconstituted α1,2-mannosidase. The reaction was incubated at 37 °C overnight.

RESULTS

Preparation of the Trisaccharide Intermediate Using Alg1. The chemoenzymatic preparation of Man-β1,4-GlcNAc-β1,4-GlcNAc-PP-Dol began with the degradation of chitin and subsequent modification to yield peracetylated chitobiose using published procedures (*37*). The remaining steps leading to dolichylpyrophosphate-linked chitobiose were also carried out as described previously (*38*). The construct used for Alg1 expression included a C-terminal His tag for purification. In addition, a V5 epitope, which is a 14 amino acid sequence from the P and V proteins of the paramyxovirus (*39*), was included at the C terminus for detection by Western blot analysis. Thus, Alg1 was overexpressed in *S. cerevisiae* and purified by Ni−NTA affinity chromatography. To analyze the reaction of Alg1 with $GlcNAc_2$-PP-Dol, dolichylpyrophosphate-linked glycans were isolated by extraction into a $CHCl_3$/MeOH layer, released from dolichylpyrophosphate by mild acid hydrolysis, and derivatized with 2-AB (*33*). Labeled glycans were then separated by normal-phase HPLC with fluorescence detection using the column specified for 2-AB-labeled glycan separation (Prozyme, Inc.) (*34*). Alg1 was able to convert the disaccharide to the trisaccharide in a greater than 95% yield, as estimated by the relative HPLC peak intensities (Figure 2). The product was confirmed by MALDI−MS of the hydrolyzed product (expected $[M + Na]^+ = 729.5$ and found $[M + Na]^+ = 729.4$).

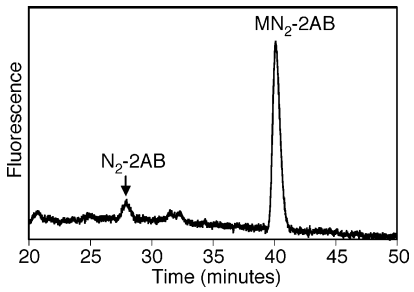

FIGURE 2: Chemoenzymatic preparation of $ManGlcNAc_2$-PP-Dol using purified Alg1. Fluorescence-based HPLC trace of approximately 5−20 pmol of extracted Alg1 products from $ManGlcNAc_2$-PP-Dol preparation, following hydrolysis and labeling with 2-AB as described in the Experimental Procedures (M, Man; N, GlcNAc; 2AB, 2-aminobenzamide).

Expression and Isolation of TRX-Alg2 and TRX-Alg11. Before the cell-membrane fraction was employed for the isolation of Alg2, other expression and purification strategies were attempted in an effort to obtain Alg2 in an active form. First, an N-terminal His-tagged Alg2 construct failed to express in *E. coli*. Expression of yeast genes in *E. coli* is often complicated by the difference in codon usage between these two organisms. In the yeast *ALG2* sequence, 35 of the 504 codons (6.9%) are considered "rare", because of the significant under representation of these codons in the coding sequence of the *E. coli* genome. Appending thioredoxin to the N terminus of sequences has been shown to improve expression and solubility of many protein targets (*40*). An Alg2 construct with an N-terminal TRX domain was thus successfully expressed in *E. coli* and purified, but no activity was detected using a very sensitive radiolabeled GDP-[^{3}H]-Man-based assay (*32*). Similar attempts to purify Alg2 activity were made using an Alg2 construct expressed in the native host, *S. cerevisiae*, which therefore did not require the TRX tag for expression. This strategy also failed to yield any detectable activity upon purification (refer to the Supporting Information for further details of these strategies).

On the basis of the apparent instability of Alg2, it was thus hypothesized that the two remote pairs of predicted transmembrane domains might rely on the membrane environment to maintain the proper structure and function of the soluble portion of the enzyme. In other words, taking Alg2 away from the membrane may be challenging the isolation of a catalytically active preparation. To test this, it was necessary to examine the activity of Alg2 while maintaining the protein in a membrane environment. However, it is critical to be able to distinguish both Alg2 and Alg11 functions from the rest of the dolichol pathway components to unambiguously define the functions of these enzymes. Therefore, expression in *E. coli* provides an ideal platform, because there are no dolichol pathway homologues in this organism. The *E. coli* cell-membrane fraction was therefore chosen as a "vehicle" for preserving the membrane environment of Alg2 and Alg11 while offering a heterologous system to enable the assignment of function. The construct chosen to test this strategy was the TRX-Alg2-V5-His fusion protein used previously for purification. After overexpression in *E. coli*, cells were harvested and lysed in the absence of detergent. Using differential centrifugation, this construct was then isolated in the cell-membrane fraction. To assess the requirement of the N-terminal TRX domain in this strategy, two Alg2 constructs were expressed and

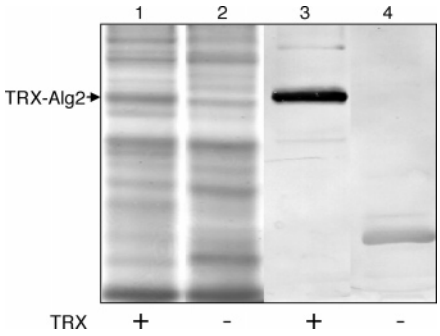

FIGURE 3: Isolated TRX-Alg2 and His-Alg2 from *E. coli* expression. Equivalent amounts of cell-membrane fraction were used for SDS−PAGE and Western blot analysis. Gelcode protein stain (Pierce Co.) of membrane fractions from the expression of TRX-Alg2-V5-His (lane 1) and His-Alg2 (lane 2) and Western blot analysis of TRX-Alg2-V5-His (lane 3) and His-Alg2 (lane 4). The Western blot was visualized using an antibody to the His tag (GE Healthcare Bio-Sciences Co.).

isolated, one with the N-terminal TRX domain and C-terminal His and V5 epitope tags and the other with only an N-terminal His tag. Levels of protein expression and isolation were compared using an antibody to the His tag. Figure 3 shows that TRX-Alg2-V5-His was successfully expressed and isolated in the cell-membrane fraction (lane 3), while in the absence of the TRX domain (lane 4), no full-length Alg2 was detected and only a smaller product, presumably a truncation product, was observed. Thus, consistent with previous observations, the TRX was crucial for expression, and therefore, the TRX-Alg2 construct was chosen for the study of the Alg2 function. Because this isolation procedure does not include affinity purification, the construct was simplified by incorporating a stop codon at the 3′ end of the *ALG2* sequence to eliminate the C-terminal tags, considering that Alg1 has been shown to be sensitive to perturbation of the C terminus (*27*). Although both constructs exhibited catalytic activity, only characterization of the construct omitting the C-terminal tags is described herein.

TRX-Alg2 Elongates ManGlcNAc$_2$-PP-Dol to Man$_3$GlcNAc$_2$-PP-Dol. The membrane fraction containing TRX-Alg2 was assayed for activity with ManGlcNAc$_2$-PP-Dol in the presence of GDP-Man as described in the Experimental Procedures. The reaction was analyzed by fluorescence-detected HPLC as described for the Alg1 reaction. Incubation with ManGlcNAc$_2$-PP-Dol in the presence of GDP-Man led to the appearance of one new major peak in the HPLC trace, corresponding to the retention time of authentic Manα1,6-(Manα1,3)-Manβ1,4-GlcNAcβ1,4-GlcNAc-2AB, and a minor peak with the retention time of authentic Manα1,3-Manβ1,4-GlcNAcβ1,4-GlcNAc-2AB (Figure 4A). To approximate the level of activity and establish enzyme dependence, radioactivity-based assays were used (Figure S1 in the Supporting Information) (*32*). To preclude the possibility that the products observed were the result of background *E. coli* enzymes or extracted native lipids, the experiment was repeated in a manner that is similar to using an empty vector control. However, instead of removing the gene, *ALG2* was replaced with *ALG11*, which would not be expected to accept the trisaccharide intermediate. Indeed, a membrane fraction containing TRX-Alg11 did not show any evidence of the reaction with the trisaccharide intermediate (Figure 4B).

Subjecting the products of the TRX-Alg2 reaction to analysis by MALDI−MS confirmed the identities of the

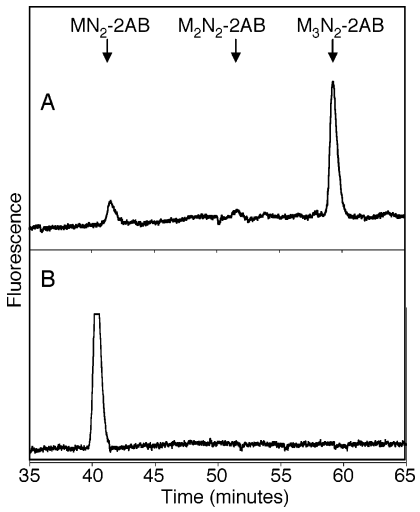

FIGURE 4: TRX-Alg2 and not TRX-Alg11 elongates ManGlcNAc$_2$-PP-Dol to Man$_3$GlcNAc$_2$-PP-Dol. Fluorescence-based HPLC traces show labeled products from reaction mixtures including ManGlcNAc$_2$-PP-Dol, GDP-Man, and the cell-membrane fraction containing (A) TRX-Alg2 or (B) TRX-Alg11. The retention times of the TRX-Alg2 products (A) match those of Man$_2$GlcNAc$_2$-2AB and Man$_3$GlcNAc$_2$-2AB authentic standards. These authentic standards have the structures of the corresponding tetra- and pentasaccharide intermediates in the dolichol pathway, respectively (retention times can vary from run to run; however, the variation is minor relative to the separation of distinct glycans) (M, Man; N, GlcNAc; 2AB, 2-aminobenzamide).

products as the tetrasaccharide, Man$_2$GlcNAc$_2$-2AB (expected $[M + H]^+ = 869.3$ and found $[M + H]^+ = 869.4$), and the pentasaccharide, Man$_3$GlcNAc$_2$-2AB (expected $[M + H]^+ = 1031.4$ and found $[M + H]^+ = 1031.3$) (Figure S2 in the Supporting Information), suggesting that Alg2 catalyzes the addition of two mannose residues. To confirm that these saccharides have the same structure as the dolichol pathway intermediates, the glycosidic linkages were mapped by specific mannosidase treatment using an α1−2,3-mannosidase from *X. manihotus* and an α1,6-mannosidase from *Xanthomonas* sp. (*41*). Treatment of the pentasaccharide (Figure 5A) with the α1−2,3-mannosidase yielded a tetrasaccharide (Figure 5B), which was sensitive to the α1,6-mannosidase (Figure 5C). These cleavage products were also confirmed by MALDI−MS (Figure S3 in the Supporting Information). The tetrasaccharide intermediate formed in trace amounts in the TRX-Alg2 reaction was shown to be sensitive to an α1−2,3-mannosidase to yield a trisaccharide (Figure 6).

These glycoside linkage-mapping results are consistent with previous analysis of accumulated dolichylpyrophosphate-linked intermediates in wild-type and mutant yeast strains. These studies had shown that the order of addition of mannose residues proceeds by α1,3-mannosylation of the trisaccharide intermediate, followed by α1,6-mannosylation of the β1,4-linked mannose residue to yield the branched core pentasaccharide product (Figure 1) (*26*, *42*).

The pentasaccharide, Man$_3$GlcNAc$_2$-2AB, was resistant to the α1,6-mannosidase (Figure S4 in the Supporting Information), which was expected because this mannosidase is incapable of catalyzing the cleavage of branched structures (*41*). This result supports the branched structure of the pentasaccharide, in accordance with the natural pentasaccharide intermediate. The only other possible structure based

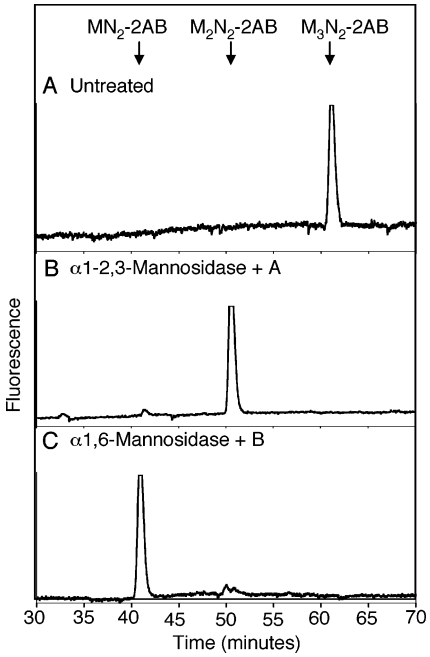

FIGURE 5: Mannosidase mapping of $Man_3GlcNAc_2$-2AB from TRX-Alg2. Fluorescence-based HPLC traces of the (A) pentasaccharide product of TRX-Alg2, $Man_3GlcNAc_2$-2AB, collected from the HPLC separation of the labeled reaction mixture, (B) product of α1−2,3-mannosidase treatment of $Man_3GlcNAc_2$-2AB, and (C) product of α1,6-mannosidase treatment of the tetrasaccharide cleavage product of $Man_3GlcNAc_2$-2AB. Cleavage reactions were carried out as described in the Experimental Procedures (M, Man; N, GlcNAc; 2AB, 2-aminobenzamide).

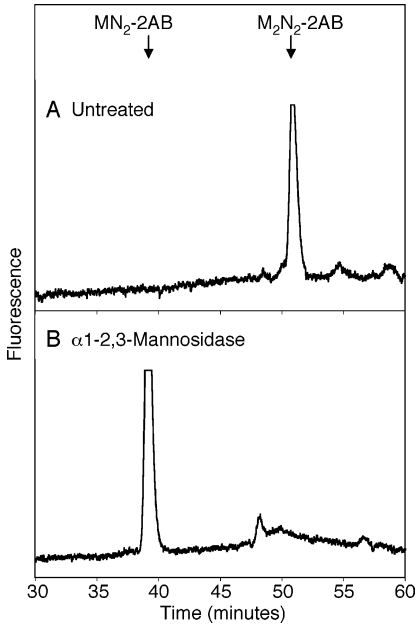

FIGURE 6: Mannosidase mapping of $Man_2GlcNAc_2$-2AB from TRX-Alg2. Fluorescence-based HPLC traces of the (A) tetrasaccharide intermediate from the TRX-Alg2 reaction, $Man_2GlcNAc_2$-2AB, collected from the HPLC separation of the labeled reaction mixture and (B) cleavage product from the treatment of the tetrasaccharide with α1−2,3-mannosidase as described in the Experimental Procedures (M, Man; N, GlcNAc; 2-AB, 2-aminobenzamide).

on the pentasaccharide linkage analysis would be a linear structure in which the α1,6-Man is in the penultimate position and the terminal mannose is α1−3 (or α1−2)-linked. However, the demonstration of the tetrasaccharide intermediate that bears a terminal α1−3 (or α1−2) linkage negates this possibility. In addition, while the α1−2,3-mannosidase does not necessarily distinguish between α1,2 and α1,3 linkages, prior knowledge of the structure of the pentasaccharide intermediate in the dolichol pathway as well as the established role of Alg2 in the early steps of the tetradecasaccharide biosynthesis support the presence of an α1,3-linked mannose and a branching of the α1,6-linked mannose from the β1,4-linked mannose. When these results are taken together, they suggest that TRX-Alg2 catalyzes the mannosylation of Manβ1,4-GlcNAcβ1,4-GlcNAc-PP-Dol to produce Manα1,3-(Manα1,6)-Manβ1,4-GlcNAcβ1,4-GlcNAc-PP-Dol via the intermediate, Manα1,3-Manβ1,4-GlcNAcβ1,4-GlcNAc-PP-Dol.

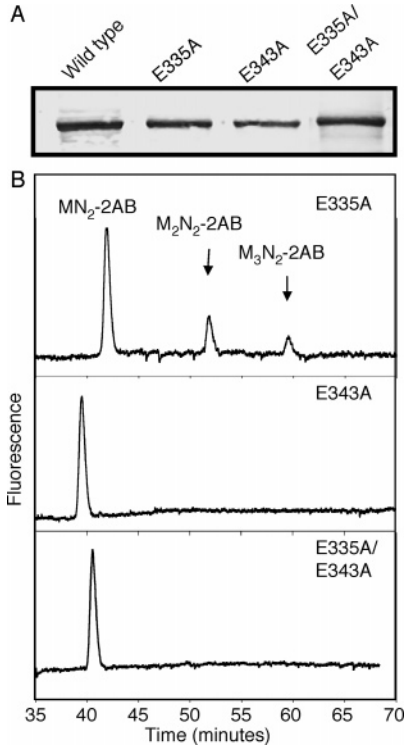

FIGURE 7: Analysis of expression/isolation and activity of TRX-Alg2 mutants. (A) Western blot analysis showing relative amounts of wild-type TRX-Alg2 (40 μg of total protein) and equivalent amounts of TRX-Alg2 mutants in cell-membrane fractions. Proteins were detected using an antibody to the TRX domain (Invitrogen). (B) Fluorescence-based HPLC traces show the results of incubating $ManGlcNAc_2$-PP-Dol with equivalent amounts (5 μL aliquots) of the TRX-Alg2 mutants E335A (top), E343A (middle), or the double mutant, E335A/E343A (bottom), prepared as described in the Experimental Procedures (M, Man; N, GlcNAc; 2AB, 2-aminobenzamide).

Analysis of Site-Directed TRX-Alg2 Mutants. The single site-directed mutants, TRX-Alg2 E335A and TRX-Alg2 E343A, as well as the double mutant, TRX-Alg2 E335A/E343A were constructed to determine the importance of the conserved glutamic acid residues in the EX_7E motif of the signature sequence and also to provide further controls to support the specific role of TRX-Alg2 in the observed activity. The relative expression/isolation levels of each mutant in comparison to wild-type TRX-Alg2 are shown in Figure 7A. It has been proposed that the first Glu residue of this motif directly participates in catalysis (*43*). Indeed, in the case of one member of this family, mutation of the first Glu residue of the EX_7E motif completely abolished activity,

while residual activity could be seen upon mutation of the second Glu residue but only in a more sensitive in vivo assay (*44*). Many more examples of probing this motif in glycosyltransferases are needed before the relative importance of the Glu residues can be generally assigned. Nevertheless, the Alg2 E335A mutation was expected to affect activity, and, indeed, a significantly lower level of product formation was observed (top of Figure 7B). More notable, however, is that the tetrasaccharide intermediate formed ($[M + Na]^+ = 890.9$; $[M + K]^+ = 906.7$) (Figure S5A in the Supporting Information) is present in greater proportion than the pentasaccharide product. Investigation of the kinetics of these reactions will be necessary to ascertain whether the mutation of the first Glu residue indeed impairs the second mannosylation step more severely than the first.

To ensure that the tetrasaccharide intermediate formed was the natural intermediate in the pathway and that the mutation did not cause the α1,6-mannosylation to occur first, the labeled tetrasaccharide product, $Man_2GlcNAc_2$-2AB, was shown to be sensitive to the α1−2,3-mannosidase and resistant to the α1,6-mannosidase (parts B and C of Figure S5 in the Supporting Information). The second Glu mutant, E343A, did not show any detectable activity (middle of Figure 7B). From this assay, it is impossible to know whether this mutation affects both steps or only the first mannosylation. In an attempt to address this issue, the E335A and E343A single mutants were assayed together. If the latter mutant was able to carry out the α1,6-mannosylation, then the combination of these mutants should yield the pentasaccharide product. However, the only product formation observed was identical to that of the E335A mutant alone (data not shown). As expected, on the basis of the results from the E343A mutant, the double mutant also does not exhibit any detectable level of product formation (bottom of Figure 7B). These mutants, while providing preliminary insight into the possible role of this motif, were prepared with the main objective of providing additional controls to confirm that the observed activity can indeed be attributed to TRX-Alg2 and not to native enzymes in the bacterial membrane fraction.

TRX-Alg11 Accepts Pentasaccharide To Form Heptasaccharide. Assigning the function of Alg11 has been hampered by the difficulty in accessing the dolichylpyrophosphate-linked penta- or hexasaccharide intermediates, which are challenging synthetic targets. Having the means to prepare the pentasaccharide intermediate chemoenzymatically using TRX-Alg2 presented the opportunity to examine the function of Alg11. TRX-Alg11 was expressed and isolated in the membrane fraction of *E. coli*, repeating exactly the methods used for TRX-Alg2. The products of the TRX-Alg2 reaction were used as starting material for elongation assays with TRX-Alg11. The starting material was thus represented by a majority of the pentasaccharide, but also contained minor amounts of tris- and tetrasaccharides (Figure 8A), and was prepared by scaling up the TRX-Alg2 reaction and then aliquoting equal amounts of the products to be used as TRX-Alg11 substrates.

Incubation of the TRX-Alg2 product mixture with TRX-Alg11 resulted in the disappearance of the pentasaccharide peak with a concomitant appearance of a peak with the retention time of the authentic heptasaccharide intermediate (Figure 8B). The heptasaccharide product was confirmed by

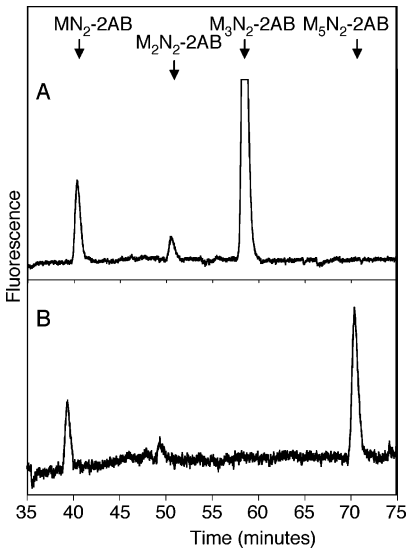

FIGURE 8: HPLC of the TRX-Alg11 product. Fluorescence-based HPLC traces show (A) TRX-Alg2 products (starting material for the TRX-Alg11 reaction) and (B) TRX-Alg11 products. A 5 μL aliquot (140 μg of total protein) of the membrane fraction bearing TRX-Alg11 was used in the elongation assay (M, Man; N, GlcNAc; 2AB, 2-aminobenzamide).

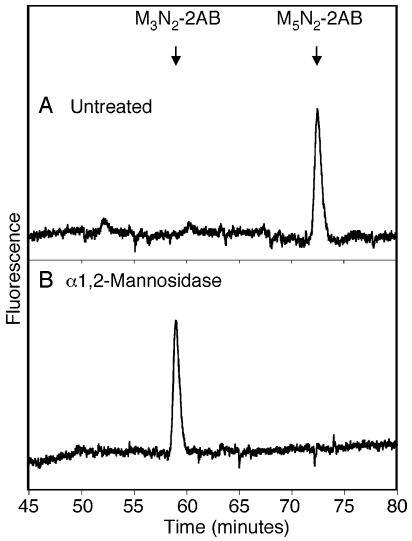

FIGURE 9: Structural characterization of the TRX-Alg11 product. Fluorescence-based HPLC traces of the heptasaccharide collected from HPLC separation of the labeled TRX-Alg11 reaction mixture (A) before and (B) after treatment with an α1,2-mannosidase (Prozyme, Inc.) as described in the Experimental Procedures (M, Man; N, GlcNAc; 2AB, 2-aminobenzamide).

MALDI−MS (expected $[M + Na]^+ = 1377.5$, found $[M + Na]^+ = 1377.5$) (Figure S6 in the Supporting Information), and the structure was characterized by cleavage with an α1,2-mannosidase from *A. saitoi* as described in the Experimental Procedures to yield a pentasaccharide (Figure 9).

These linkage-mapping results are consistent with the expected structure, Manα1,2-Manα1,2-Manα1,3-(Manα1,6)-Manβ1,4-GlcNAcβ1,4-GlcNAc-2AB. Thus, TRX-Alg11 was shown to catalyze the elongation of Manα1,3-(Manα1,6)-Manβ1,4-GlcNAcβ1,4-GlcNAc-PP-Dol to Manα1,2-Manα1,2-Manα1,3-(Man-α1,6)-Man-β1,4-GlcNAcβ1,4-GlcNAc-PP-Dol. The residual tri- and tetrasaccharide intermediates remained unreacted, highlighting the specificity of TRX-Alg11 and providing more convincing evidence that the

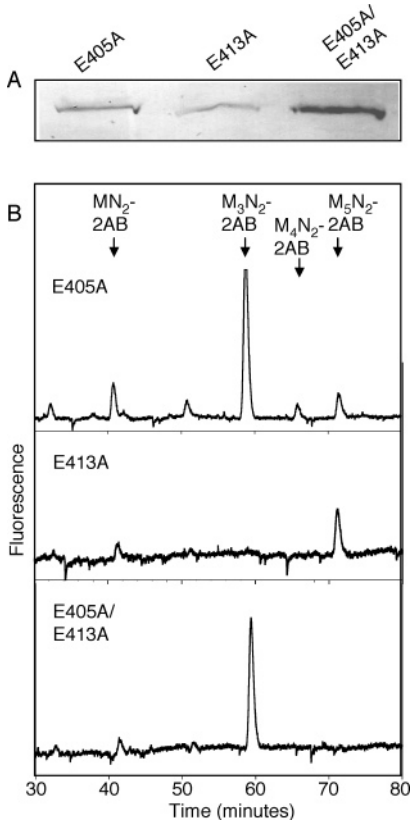

FIGURE 10: Analysis of expression and activity of TRX-Alg11 mutants. (A) Western blot analysis of equivalent amounts of cell-membrane fraction from the overexpression of all TRX-Alg11 mutants to show relative expression levels, with α-Thio (Invitrogen) detection of the TRX domain. (B) Fluorescence-based HPLC traces show the results of incubating $Man_3GlcNAc_2$-PP-Dol with equivalent amounts (5 μL aliquots) of the TRX-Alg11 mutants E405A (top), E413A (middle), or the double mutant, E405A/E413A (bottom), prepared as described in the Experimental Procedures (M, Man; N, GlcNAc; 2AB, 2-aminobenzamide).

pentasaccharide is the substrate of Alg11. The fact that the TRX-Alg2 membrane fraction does not elongate the pentasaccharide product further provides evidence that precludes the possibility of native *E. coli* enzymes completing the heptasaccharide biosynthesis.

Mannosyltransferase Activities of TRX-Alg11 Mutants. Further evidence that the observed activity was specific to TRX-Alg11 was sought through the use of point mutations of the conserved Glu residues in the signature sequence, as was done for TRX-Alg2. The relative expression/isolation levels of the three mutants were evaluated by Western blot analysis (Figure 10A). The levels of all mutants were lower than wild-type TRX-Alg11; however, the results of the mutations range from product formation comparable to that of the wild-type sequence to no detection of product formation and, thus, can be compared independently of the wild-type activity. Mutation of the first Glu residue (TRX-Alg11 E405A) caused nearly complete abrogation of product formation, with only trace amounts observed by HPLC (top of Figure 10B). These trace products were subjected to α1,2-mannosidase cleavage to identify them as the expected hexa- and heptasaccharide products, $Man_4GlcNAc_2$-PP-Dol and $Man_5GlcNAc_2$-PP-Dol, respectively (Figure S7 in the Supporting Information). In contrast, the degree of product formation achieved by the TRX-Alg11 E413A mutant was indistinguishable from that of the wild-type enzyme under comparable conditions (middle of Figure 10B), which is consistent with previous hypotheses that the first Glu residue of the EX_7E motif is more critical for activity. For reasons that are unclear at the current time, the double mutant is consistently expressed (or isolated) at a significantly higher level compared to the single mutants. This characteristic, however, does not complicate the interpretation of the elongation assay results, because no product formation was detected in an elongation assay with this mutant. The complete loss of activity in the double mutant, TRX-Alg11 E405A/E413A (bottom of Figure 10B), suggests that either the E413 is critical for the residual activity displayed by the E405A mutant or perhaps this perturbation in local structure is enough to abolish the remaining activity. More importantly, in terms of the current goal of defining the precise function of Alg11, the sensitivity of the observed activity to point mutations in TRX-Alg1l and, particularly, the complete loss of activity in the double mutant, despite robust expression, argues against any involvement of native *E. coli* enzymes in the cell-membrane fraction.

Specificity of TRX-Alg2 and TRX-Alg11. In the interest of unambiguously assigning the function of Alg2 and Alg11 from these studies, it was necessary to show that each is specific for the proposed substrate. To demonstrate that Alg2 and Alg11 are capable of distinguishing the correct substrate from preceding intermediates in the pathway, different combinations of Alg1 from *S. cerevisiae* expression, TRX-Alg2, and TRX-Alg11 were incubated with the Alg1 substrate, $GlcNAc_2$-PP-Dol. In the absence of Alg1, there was no evidence of elongation of $GlcNAc_2$-PP-Dol, demonstrating that neither TRX-Alg2 nor TRX-Alg11 accepts this intermediate (Figure 11A). In the absence of TRX-Alg2, $ManGlcNAc_2$-PP-Dol accumulates, showing that TRX-Alg11 also does not accept the trisaccharide intermediate (Figure 11B). The complete elongation to $Man_5GlcNAc_2$-PP-Dol in the presence of Alg1, TRX-Alg2, and TRX-Alg11 confirmed that all components were active and that these three enzymes are sufficient to carry out all five mannosylation steps of the dolichol pathway that occur on the cytosolic face of the ER membrane (Figure 11C).

DISCUSSION

The results presented in this paper demonstrate the dual function of Alg2 and Alg11, which complement the recent evidence for the dual function of Alg9 and, thus, complete the identification of the entire ensemble of glycosyltransferases that comprise the dolichol pathway. These findings explain the absence of candidates for these steps generated through genetic screens and bioinformatic approaches. Similar examples of this paradox, in which too few candidate glycosyltransferases are available to account for all of the steps in a biosynthetic pathway, have recently been found in *Streptomyces cyanogenus* and in *Campylobacter jejuni* (*45*, *46*). In *S. cyanogenus*, landomycin A biosynthesis involves the assembly of a hexasaccharide moiety by two monofunctional and two bifunctional glycosyltransferases (*45*). The Pgl pathway of N-linked protein glycosylation in *C. jejuni* has many similarities to the dolichol pathway, including the assembly of a polyisoprenoid pyrophosphate-linked oligosaccharide as the donor for transfer to protein (*47*). Within the Pgl pathway, the α1,4-*N*-acetylgalactosaminyltransferase, PglH, acts iteratively to transfer three GalNAc residues to

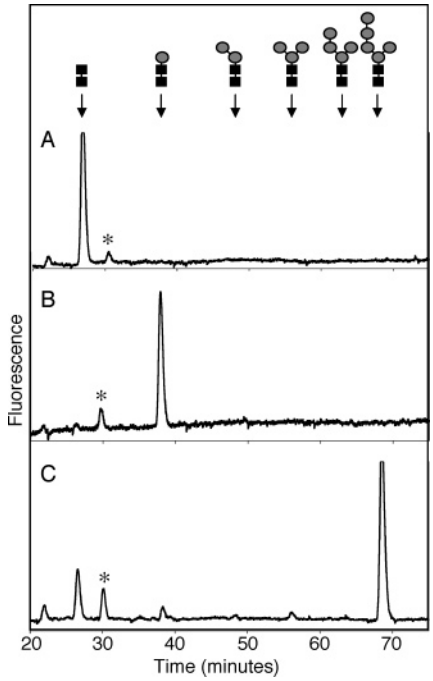

FIGURE 11: Specificity of TRX-Alg2 and TRX-Alg11. Fluorescence-based HPLC traces of hydrolyzed and 2-AB-labeled reaction mixtures following $GlcNAc_2$-PP-Dol elongation with different permutations of Alg1 (0.13 μg, purified), TRX-Alg2 (200 μg of total protein, membrane fraction), and TRX-Alg11 (50 μg of total protein, membrane fraction). (A) TRX-Alg2 + TRX-Alg11. (B) Alg1 + TRX-Alg11 (C) Alg1 + TRX-Alg2 + TRX-Alg11. (*) Uncharacterized impurity has the retention time of peracetylated $GlcNAc_2$-2AB (gray circles, Man; black squares, GlcNAc; structures represent hydrolyzed and 2-aminobenzamide-labeled products).

the growing oligosaccharide chain (*46*). In these two examples, as in the case of Alg11, the enzymes are transferring the same sugar to form the same glycosidic linkage.

Other examples of bifunctional glycosyltransferases include the chondroitin synthases, which display both β1,3-*N*-acetylgalactosamine transferase and β1,4-glucuronic acid transferase activities (*48*−*52*), and hyaluronan synthase (*52*, *53*), having β1,3-*N*-acetylglucosamine transferase and β1,4-glucuronic acid transferase activities. The enzyme FT85 from *Dictyostelium* displays both β1,3-galactosytransferase and α1,2-fucosyltransferase activities (*54*), and the *E. coli* enzyme, KfiC, polymerizes a repeat structure of a bacterial capsular polysaccharide by alternating α1,4 and β1,4 additions of *N*-acetylglucosamine and glucuronic acid, respectively (*55*). A common feature of all of these bifunctional glycosyltransferases is the apparent presence of two separate glycosyltransferase domains that isolate the two distinct activities. This characteristic may be necessary because of the fact that, unlike Alg2 and Alg11, two different types of glycosyl donors must be recognized. These bifunctional enzymes are also significantly larger than Alg2 and Alg11.

The results of the Alg2 mutants presented here suggest that only one active site is used for both transformations, because the first Glu residue of the EX_7E motif seems to be important for the α1,6-mannosylation and the second Glu residue affects (at least) the α1,3-mannosylation. Similarly, in the case of Alg11, mutation of the first Glu residue appears to affect both of the α1,2-mannosylations for which it is responsible. Total product formation is markedly lower with the E405A mutant, and the observed accumulation of the hexasaccharide intermediate suggests that the second step is also impaired.

Despite the low-sequence homology, there is a great deal of structural homology among glycosyltransferases for which structures have been determined (*29*). There are two major folds, known as GT-A and GT-B, among several glycosyltransferase families (*56*). The GT-B fold is characterized by two dissimilar subdomains separated by a hinge region, one of which is responsible for binding the nucleotide sugar, while the other binds the acceptor (*43*). Structures have been solved by X-ray analysis for three of the glycosyltransferases that include the previously mentioned conserved signature sequence, including MurG, GtfB, and β-GT (*57*−*59*). All of these structures reveal a GT-B fold and involvement of the conserved residues in binding of the nucleotide-sugar donor. MurG, like enzymes in the dolichol pathway, is membrane-associated, and the glycosyl acceptor is activated by a long-chain pyrophosphate-linked polyisoprene. In Alg2 and Alg11, the conserved signature sequence lies within the soluble cytosolic region. Threading analysis with sequences of glycosyltransferases for which structures have not been solved reveal that most fall within either the GT-A or GT-B fold family. Selected sequences from the Pfam family, to which Alg2 and Alg11 belong, were analyzed by threading analysis and were predicted to adopt the GT-B fold (*60*). For all of these reasons, it is suspected that Alg2 and Alg11 may also adopt the GT-B fold, separating the two substrate binding sites by a flexible loop.

As increasing numbers of glycosyltransferase structures are available, there is mounting evidence that the nucleotide-sugar donor utilizing glycosyltransferases have a flexible loop above the donor-binding site that closes upon donor binding, creating the binding site of the acceptor (*61*). Plasticity of the active site and the flexibility between acceptor- and donor-binding sites may help to explain how enzymes with the same overall structure are used for the formation of more than one type of glycosidic linkage and for the transfer of more than one monosaccharide. It has been shown that constraining glycosyl acceptors into a variety of conformations can have a significant impact on the kinetic parameters of the glycosyltransferases that recognize them (*62*). Much more work is needed to begin to understand how Alg2 can carry out an α1,3-mannosylation when the trisaccharide intermediate is bound, while binding of the tetrasaccharide induces an α1,6-mannosylation, thus changing the linkage specificity by changing the substrate.

CONCLUSIONS

In vitro biochemical studies presented herein provide evidence for the dual function of both Alg2 and Alg11, thus laying the groundwork for future studies of the coordinated actions of these enzymes. Glycosyltransferases are notoriously unstable and are often membrane-associated. Thus, the challenges in studying the dolichol pathway from a biochemical standpoint have also hindered progress toward obtaining a complete mechanistic picture of glycosyltransferases. The work described here demonstrates the utility of an alternative method for isolating the activity of single dolichol pathway enzymes while maintaining a nativelike membrane environment. Future work will be necessary to

gain kinetic information about these enzymes to understand how two mannosyltransferase steps can occur, particularly with two different linkage specificities, as well as the role of the conserved glutamate residues. Finally, just as the chemoenzymatic preparation of the core trisaccharide has been accomplished (*21*), it is now possible to prepare both the core pentasaccharide and the full heptasaccharide product of the cytosolic transferases using a chemoenzymatic approach.

ACKNOWLEDGMENT

We thank Langdon Martin and Dr. Matthieu Sainlos for obtaining the MALDI−MS data, Dr. Eranthie Weerapana for providing assistance with synthesis, Professor Neta Dean for the NDY13.4 yeast strain, and Professor Maria Kukuruzinska for the *alg2* temperature-sensitive yeast strain.

SUPPORTING INFORMATION AVAILABLE

Experimental procedures for the cloning of all constructs; expression and purification of Alg1 and inactive Alg2 constructs; radioactive activity assays showing enzyme dependence of TRX-Alg2; MALDI−MS data; and fluorescence HPLC traces of additional characterization by mannosidase treatment. This material is available free of charge via the Internet at http://pubs.acs.org.

REFERENCES

1. Kornfeld, R., and Kornfeld, S. (1985) Assembly of asparagine-linked oligosaccharides, *Annu. Rev. Biochem. 54*, 631−664.
2. Imperiali, B. (1997) Protein glycosylation: The clash of the titans, *Acc. Chem. Res. 30*, 452−459.
3. Kelleher, D. J., and Gilmore, R. (2005) An evolving view of the eukaryotic oligosaccharyltransferase, *Glycobiology 16*, 47R−62R.
4. Burda, P., and Aebi, M. (1999) The dolichol pathway of N-linked glycosylation, *Biochim. Biophys. Acta 1426*, 239−257.
5. Cipollo, J. F., Trimble, R. B., Chi, J. H., Yan, Q., and Dean, N. (2001) The yeast ALG11 gene specifies addition of the terminal α1,2-Man to the Man5GlcNAc2-PP-dolichol N-glycosylation intermediate formed on the cytosolic side of the endoplasmic reticulum, *J. Biol. Chem. 276*, 21828−21840.
6. Cipollo, J. F., and Trimble, R. B. (2002) The *Saccharomyces cerevisiae* alg12Δ mutant reveals a role for the middle-arm α1,-2Man- and upper-arm α1,2Manα1,6Man- residues of Glc3Man9-GlcNAc2-PP-Dol in regulating glycoprotein glycan processing in the endoplasmic reticulum and Golgi apparatus, *Glycobiology 12*, 749−762.
7. Chantret, I., Dancourt, J., Barbat, A., and Moore, S. E. (2005) Two proteins homologous to the N- and C-terminal domains of the bacterial glycosyltransferase MurG are required for the second step of dolichyl-linked oligosaccharide synthesis in *Saccharomyces cerevisiae*, *J. Biol. Chem. 280*, 9236−9242.
8. Frank, C. G., and Aebi, M. (2005) ALG9 mannosyltransferase is involved in two different steps of lipid-linked oligosaccharide biosynthesis, *Glycobiology 15*, 1156−1163.
9. Hirschberg, C. B., and Snider, M. D. (1987) Topography of glycosylation in the rough endoplasmic reticulum and Golgi apparatus, *Annu. Rev. Biochem. 56*, 63−87.
10. Abeijon, C., and Hirschberg, C. B. (1992) Topography of glycosylation reactions in the endoplasmic reticulum, *Trends Biochem. Sci. 17*, 32−36.
11. Helenius, J., Ng, D. T., Marolda, C. L., Walter, P., Valvano, M. A., and Aebi, M. (2002) Translocation of lipid-linked oligosaccharides across the ER membrane requires Rft1 protein, *Nature 415*, 447−450.
12. Rine, J., Hansen, W., Hardemann, E., and Davis, R. W. (1983) Targeted selection of recombinant clones through gene dosage effects, *Proc. Natl. Acad. Sci. U.S.A. 80*, 6750−6754.
13. Bickel, T., Lehle, L., Schwarz, M., Aebi, M., and Jakob, C. A. (2005) Biosynthesis of lipid-linked oligosaccharides in *Saccharomyces cerevisiae*: Alg13p and Alg14p form a complex required for the formation of GlcNAc(2)-PP-dolichol, *J. Biol. Chem. 280*, 34500−34506.
14. Gao, X. D., Tachikawa, H., Sato, T., Jigami, Y., and Dean, N. (2005) Alg14 recruits Alg13 to the cytoplasmic face of the endoplasmic reticulum to form a novel bipartite UDP-*N*-acetylglucosamine transferase required for the second step of N-linked glycosylation, *J. Biol. Chem. 280*, 36254−36262.
15. Huffaker, T. C., and Robbins, P. W. (1982) Temperature-sensitive yeast mutants deficient in asparagine-linked glycosylation, *J. Biol. Chem. 257*, 3203−3210.
16. Couto, J. R., Huffaker, T. C., and Robbins, P. W. (1984) Cloning and expression in *Escherichia coli* of a yeast mannosyltransferase from the asparagine-linked glycosylation pathway, *J. Biol. Chem. 259*, 378−382.
17. Albright, C. F., and Robbins, P. W. (1990) The sequence and transcript heterogeneity of the yeast gene ALG1, an essential mannosyltransferase involved in N-glycosylation, *J. Biol. Chem. 265*, 7042−7049.
18. Wilson, I. B., Webberley, M. C., Revers, L., and Flitsch, S. L. (1995) Dolichol is not a necessary moiety for lipid-linked oligosaccharide substrates of the mannosyltransferases involved in in vitro N-linked-oligosaccharide assembly, *Biochem. J. 310* (part 3), 909−916.
19. Flitsch, S. L., Goodridge, D. M., Guilbert, B., Revers, L., Webberley, M. C., and Wilson, I. B. (1994) The chemoenzymatic synthesis of neoglycolipids and lipid-linked oligosaccharides using glycosyltransferases, *Bioorg. Med. Chem. 2*, 1243−1250.
20. Revers, L., Wilson, I. B., Webberley, M. C., and Flitsch, S. L. (1994) The potential dolichol recognition sequence of β-1,4-mannosyltransferase is not required for enzymic activity using phytanyl-pyrophosphoryl-α-*N*,*N*′-diacetylchitobioside as acceptor, *Biochem. J. 299* (part 1), 23−27.
21. Watt, G. M., Revers, L., Webberley, M. C., Wilson, I. B. H., and Flitsch, S. L. (1997) Efficient enzymatic synthesis of the core trisaccharide of *N*-glycans with a recombinant β-mannosyltransferase, *Angew. Chem., Int. Ed. Eng. 36*, 2354−2356.
22. Huffaker, T. C., and Robbins, P. W. (1983) Yeast mutants deficient in protein glycosylation, *Proc. Natl. Acad. Sci. U.S.A. 80*, 7466−7470.
23. Jackson, B. J., Kukuruzinska, M. A., and Robbins, P. W. (1993) Biosynthesis of asparagine-linked oligosaccharides in *Saccharomyces cerevisiae*: The *alg2* mutation, *Glycobiology 3*, 357−364.
24. Yamakazi, H., Shiraishi, N., Takauchi, K., Ohnishi, Y., and Horinouchi, S. (1998) Characterization of ALG2 encoding a mannosyltransferase in the zygomycete fungus *Rhizomucor pusillus*, *Gene 221*, 179−184.
25. Takeuchi, K., Yamazaki, H., Shiraishi, N., Ohnishi, Y., Nishikawa, Y., and Horinouchi, S. (1999) Characterization of an *alg2* mutant of the zygomycete fungus *Rhizomucor pusillus*, *Glycobiology 9*, 1287−1293.
26. Thiel, C., Schwarz, M., Peng, J., Grzmil, M., Hasilik, M., Braulke, T., Kohlschutter, A., von Figura, K., Lehle, L., and Korner, C. (2003) A new type of congenital disorder of glycosylation (CDG-II) provides new insights into the early steps of dolichol-linked oligosaccharide biosynthesis, *J. Biol. Chem. 278*, 22498−22505.
27. Gao, X.-D., Nishikawa, A., and Dean, N. (2004) Physical interactions between the Alg1, Alg2, and Alg11 mannosyltransferases of the endoplasmic reticulum, *Glycobiology 14*, 559−570.
28. Burda, P., Jakob, C. A., Beinhauer, J., Hegemann, J. H., and Aebi, M. (1999) Ordered assembly of the asymmetrically branched lipid-linked oligosaccharide in the endoplasmic reticulum is ensured by the substrate specificity of the individual glycosyltransferases, *Glycobiology 9*, 617−625.
29. Hu, Y., and Walker, S. (2002) Remarkable structural similarities between diverse glycosyltransferases, *Chem. Biol. 9*, 1287−1296.
30. Bateman, A., Coin, L., Durbin, R., Finn, R. D., Hollich, V., Griffiths-Jones, S., Khanna, A., Marshall, M., Moxon, S., Sonnhammer, E. L. L., Studholme, D. J., Yeats, C., and Eddy, S. R. (2004) The Pfam protein families database, *Nucleic Acids Res. 32*, D138−D141.
31. Krogh, A., Larsson, B., von Heijne, G., and Sonnhammer, E. L. (2001) Predicting transmembrane protein topology with a hidden Markov model: Application to complete genomes, *J. Mol. Biol. 305*, 567−580.
32. Tai, V. W.-F., O'Reilly, M. K., and Imperiali, B. (2001) Substrate specificity of *N*-acetylglucosaminyl (diphosphodolichol) *N*-acetylglucosaminyl transferase, a key enzyme in the dolichol pathway, *Bioorg. Med. Chem. Lett. 9*, 1133−1140.

33. Bigge, J. C., Patel, T. P., Bruce, J. A., Goulding, P. N., Charles, S. M., and Parekh, R. B. (1995) Nonselective and efficient fluorescent labeling of glycans using 2-amino benzamide and anthranilic acid, *Anal. Biochem. 230*, 229−238.
34. Guile, G. R., Rudd, P. M., Wing, D. R., Prime, S. B., and Dwek, R. A. (1996) A rapid high-resolution high-performance liquid chromatographic method for separating glycan mixtures and analyzing oligosaccharide profiles, *Anal. Biochem. 240*, 210−226.
35. Dean, N. (1995) Yeast glycosylation mutants are sensitive to aminoglycosides, *Proc. Natl. Acad. Sci. U.S.A. 92*, 1287−1291.
36. Hansske, B., Thiel, C., Lübke, T., Hasilik, M., Höning, S., Peters, V., Heidemann, P. H., Hoffmann, G. F., Berger, E. G., von Figura, K., and Korner, C. (2002) Deficiency of UDP-galactose: *N*-acetylglucosamine β-1,4-galactosyltransferase I causes the congenital disorder of glycosylation type IId, *J. Clin. Invest. 109*, 725−733.
37. Terayama, H., Takahashi, S., and Kuzuhara, H. (1993) Large-scale preparation of *N*,*N*′-diacetylchitobiose by enzymatic degradation of chitin and its chemical modifications, *J. Carbohydr. Chem. 12*, 81−93.
38. Lee, J., and Coward, J. K. (1992) Enzyme-catalyzed glycosylation of peptides using a synthetic lipid disaccharide substrate, *J. Org. Chem. 57*, 4126−4135.
39. Southern, J. A., Young, D. F., Heaney, F., Baumgartner, W. K., and Randall, R. E. (1991) Identification of an epitope on the P and V proteins of simian virus 5 that distinguishes between two isolates with different biological characteristics, *J. Gen. Virol. 72* (part 7), 1551−1557.
40. LaVallie, E. R., DiBlasio-Smith, E. A., Collins-Racie, L. A., Lu, Z., and McCoy, J. M. (2003) Thioredoxin and related proteins as multifunctional fusion tags for soluble expression in *E. coli*, *Methods Mol. Biol. 205*, 119−140.
41. Wong-Madden, S. T., and Landry, D. (1995) Purification and characterization of novel glycosidases from the bacterial genus *Xanthomonas*, *Glycobiology 5*, 19−28.
42. Chapman, A., Li, E., and Kornfeld, S. (1979) The biosynthesis of the major lipid-linked oligosaccharide of Chinese hamster ovary cells occurs by the ordered addition of mannose residues, *J. Biol. Chem. 254*, 10243−10249.
43. Bourne, Y., and Henrissat, B. (2001) Glycoside hydrolases and glycosyltransferases: Families and functional modules, *Curr. Opin. Struct. Biol. 11*, 593−600.
44. Abdian, P. L., Lellouch, A. C., Gautier, C., Ielpi, L., and Geremia, R. A. (2000) Identification of essential amino acids in the bacterial α-mannosyltransferase AceA, *J. Biol. Chem. 275*, 40568−40575.
45. Luzhetskyy, A., Fedoryshyn, M., Durr, C., Taguchi, T., Novikov, V., and Bechthold, A. (2005) Iteratively acting glycosyltransferases involved in the hexasaccharide biosynthesis of landomycin A, *Chem. Biol. 12*, 725−729.
46. Glover, K. J., Weerapana, E., and Imperiali, B. (2005) In vitro assembly of the undecaprenylpyrophosphate-linked heptasaccharide for prokaryotic N-linked glycosylation, *Proc. Natl. Acad. Sci. U.S.A. 102*, 14255−14259.
47. Szymanski, C. M., Logan, S. M., Linton, D., and Wren, B. W. (2003) Campylobacter—A tale of two protein glycosylation systems, *Trends Microbiol. 11*, 233−238.
48. Hwang, H. Y., Olson, S. K., Esko, J. D., and Horvitz, H. R. (2003) *Caenorhabditis elegans* early embryogenesis and vulval morphogenesis require chondroitin biosynthesis, *Nature 423*, 439−443.
49. Yada, T., Gotoh, M., Sato, T., Shionyu, M., Go, M., Kaseyama, H., Iwasaki, H., Kikuchi, N., Kwon, Y. D., Togayachi, A., Kudo, T., Watanabe, H., Narimatsu, H., and Kimata, K. (2003) Chondroitin sulfate synthase-2. Molecular cloning and characterization of a novel human glycosyltransferase homologous to chondroitin sulfate glucuronyltransferase, which has dual enzymatic activities, *J. Biol. Chem. 278*, 30235−30247.
50. Yada, T., Sato, T., Kaseyama, H., Gotoh, M., Iwasaki, H., Kikuchi, N., Kwon, Y. D., Togayachi, A., Kudo, T., Watanabe, H., Narimatsu, H., and Kimata, K. (2003) Chondroitin sulfate synthase-3. Molecular cloning and characterization, *J. Biol. Chem. 278*, 39711−39725.
51. Ninomiya, T., Sugiura, N., Tawada, A., Sugimoto, K., Watanabe, H., and Kimata, K. (2002) Molecular cloning and characterization of chondroitin polymerase from *Escherichia coli* strain K4, *J. Biol. Chem. 277*, 21567−21575.
52. Jing, W., and DeAngelis, P. L. (2003) Analysis of the two active sites of the hyaluronan synthase and the chondroitin synthase of *Pasteurella multocida*, *Glycobiology 13*, 661−671.
53. Jing, W., and DeAngelis, P. L. (2000) Dissection of the two transferase activities of the *Pasteurella multocida* hyaluronan synthase: Two active sites exist in one polypeptide, *Glycobiology 10*, 883−889.
54. van der Wel, H., Fisher, S. Z., and West, C. M. (2002) A bifunctional diglycosyltransferase forms the Fucα1,2Galβ1,3-disaccharide on Skp1 in the cytoplasm of dictyostelium, *J. Biol. Chem. 277*, 46527−46534.
55. Griffiths, G., Cook, N. J., Gottfridson, E., Lind, T., Lidholt, K., and Roberts, I. S. (1998) Characterization of the glycosyltransferase enzyme from the *Escherichia coli* K5 capsule gene cluster and identification and characterization of the glucuronyl active site, *J. Biol. Chem. 273*, 11752−11757.
56. Unligil, U. M., and Rini, J. M. (2000) Glycosyltransferase structure and mechanism, *Curr. Opin. Struct. Biol. 10*, 510−517.
57. Ha, S., Walker, D., Shi, Y., and Walker, S. (2000) The 1.9 Å crystal structure of *Escherichia coli* MurG, a membrane-associated glycosyltransferase involved in peptidoglycan biosynthesis, *Protein Sci. 9*.
58. Mulichak, A. M., Losey, H. C., Walsh, C. T., and Garavito, R. M. (2001) Structure of the UDP-glucosyltransferase GtfB that modifies the heptapeptide aglycone in the biosynthesis of vancomycin group antibiotics, *Structure 9*, 547−557.
59. Vrielink, A., Ruger, W., Driessen, H. P. C., and Freemont, P. S. (1994) Crystal structure of the DNA modifying enzyme beta-glucosyltransferase in the presence and absence of substrate uridine diphosphoglucose, *EMBO J. 13*, 3413−3422.
60. Breton, C., Snajdrova, L., Jeanneau, C., Koca, J., and Imberty, A. (2006) Structures and mechanisms of glycosyltransferases, *Glycobiology 16*, 29R−37R.
61. Qasba, P. K., Ramakrishnan, B., and Boeggeman, E. (2005) Substrate-induced conformational changes in glycosyltransferases, *Trends Biochem. Sci. 30*, 53−62.
62. Galan, M. C., Venot, A. P., and Boons, G. J. (2003) Glycosyltransferase activity can be modulated by small conformational changes of acceptor substrates, *Biochemistry 42*, 8522−8529.

BI060878O